JOURNAL OF PROPULSION AND POWER
Vol. 9, No. 6, Nov.–Dec. 1993

Cathode Phenomena in Plasma Thrusters

Monika Auweter-Kurtz,* Bernd Glocker,† Helmut L. Kurtz,‡ Otto Loesener,† Herbert O. Schrade,§
Nikolaos Tubanos,† Thomas Wegmann,† and Dieter Willer¶
Universität Stuttgart, 70550 Stuttgart, Germany
and
James E. Polk**
Princeton University, Princeton, New Jersey 08540

For the optimization of cathodes of steady-state plasma accelerators, an extensive experimental program has been carried out at IRS to investigate the erosion mechanisms. On different thruster types and with an additional fundamental experiment, the influences of geometry, chamber pressure, amount of ThO_2, cathode temperature, power, and gas species were explored. Propellants Ar, H_2, N_2 were used which had been purified with a special filter to remove residual water and oxygen. The erosion rates during the ignition phase as well as during continuous operation were measured. The temporal evolution of the cathode erosion rate was measured by surface layer activation. At high current densities within the cathode, severe problems were encountered with all thruster geometries. The cathodes developed cracks and started to melt. To clarify the reason for this behavior, some cathodes were investigated metallurgically.

I. Introduction

DUE to the lack of large space power supplies, most of the research work on the self-field magnetoplasmadynamic (MPD) thruster propulsion was concentrated in the last two decades on the pulsed quasisteady operation modes. There it showed that the erosion of the cathode was the main lifetime limiting factor of these devices. Therefore, the arc attachment and the erosion of cold cathodes were investigated thoroughly, both experimentally as well as theoretically.[1–5] In many respects the pulsed operation mode resembles the switching arc phenomena, so that the intensive research in this field has contributed much to the understanding of the erosion mechanisms of cold cathodes.[6–8] On the other hand, the research on high current thermionic cathodes was largely neglected, and a gap arose after many studies were made in the sixties,[9,10] so that in a new MPD thruster survey paper[11] only one new study[12] was cited. More recent works were confined to low-power MPD thrusters[13] and arcjets.[14,15] Now, with the prospect of deploying high-power energy supplies in space like the nuclear reactor SP-100, and with forthcoming missions such as the manned Mars missions, a renewed interest arose in steady-state, self-field MPD thrusters, and hence also in the problems of hot cathodes. The emphasis of this article is put on high-power phenomena of hot cathodes. However, since the cathode is cold at ignition, the ignition phase was also investigated in all thrusters.

During the study it was found that the erosion is determined mainly by sublimation. Using a specially designed MPD device with a freely visible cathode, the cathode temperature and erosion as a function of current were measured. The surface layer activation method (SLA), developed at Princeton University for cold cathodes,[16] was installed in the same thruster, and this measurement method confirmed the erosion values established by weighing the cathodes.

Although erosion no longer seemed to be a limiting factor, at high current densities a new failure mode emerged in which internal melting led to cathode destruction. The internal melting was not observed at the hot emitting tip, but near the base of the cathode before the attachment zone. Some damaged cathodes have been investigated metallographically and recommendations have been made to overcome this destructive behavior.

II. Facilities

The MPD accelerators used for the erosion tests are thrusters of the nozzle type DT-IRS series [Fig. 1 (Ref. 17)], and plasma generators for application in arc-heated wind tunnels RD-IRS, which have a geometry essentially similar to the DT-IRS series.[18] These MPD accelerators are concentric segmented devices with each segment water-cooled and the last one downstream switched as anode. The center cathode consists of a thoriated tungsten rod with a diameter of 8 mm for plasma generator application, and of 12–18 mm for high-

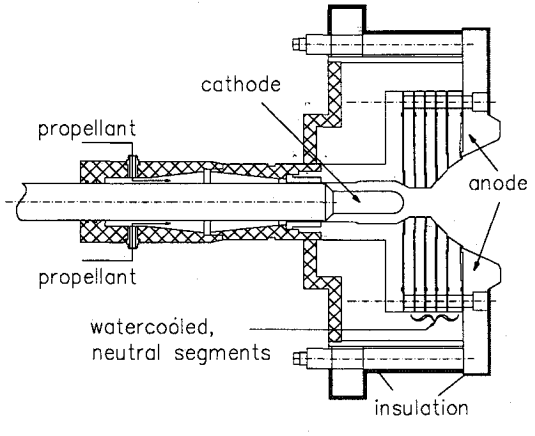

Fig. 1 Nozzle-type MPD thruster DT.

Presented as Paper 90-2662 at the AIAA/DGLR/JSASS International Electric Propulsion Conference, Orlando, FL, July 18–20, 1990; received Nov. 9, 1990; revision received Feb. 19, 1993; accepted for publication April 29, 1993.

*Professor, Institut für Raumfahrtsysteme, Pfaffenwaldring 31.
†Research Scientist, Institut für Raumfahrtsysteme, Pfaffenwaldring 31.
‡Senior Research Engineer, Institut für Raumfahrtsysteme, Pfaffenwaldring 31.
§Senior Scientist, Institut für Raumfahrtsysteme, Pfaffenwaldring 31.
¶Research Scientist, Staatliche Materialprüfungsanstalt, Universität Stuttgart, Pfaffenwaldring 32.
**Research Scientist; currently at the Jet Propulsion Laboratory, 4800 Oak Grove Drive, Pasadena, CA 91109.

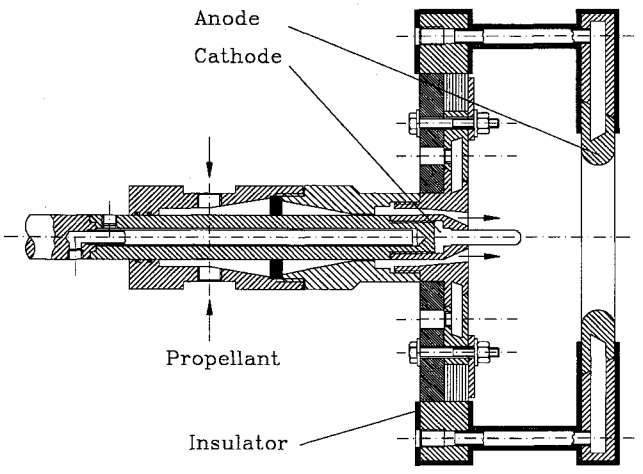

Fig. 2 MPD device DTF.

power MPD thrusters. They are either clamped (for currents <3000 A) or cast (for high-current application) into a copper base which is screwed onto a water-cooled copper rod. The clamped cathodes can be loosened easily for weighing with a balance which has an accuracy of 0.01 mg. The propellant is fed around the cathode shaft into the arc chamber.

In order to determine the distribution of temperature and current density on the cathode surface, the nozzle-type MPD thruster of type DT-IRS (Fig. 1) was modified. The MPD device DTF shown in Fig. 2 has a ring-shaped, water-cooled copper anode and a thoriated tungsten cathode, 12 mm in diameter and 65-mm long, mounted in a water-cooled copper shaft similar to the DT thruster. In this configuration, however, one has free optical access to the entire cathode rod, since the chamber and all segments except the anode have been removed. High-purity argon propellant was injected around the cathode base.

The DTF thruster was mounted in a vacuum chamber 2 m in diameter and 5-m long, capable of achieving a vacuum of about 4×10^{-3} mbar. However, to avoid preferential cathode attachment at the base and to simulate the higher pressure environment of the chamber upstream of the nozzle throat, the pressure was maintained at 15–25 mbar.

High-current experiments were conducted with the cylindrical MPD thruster ZT1-IRS described in detail in Ref. 19. The ZT1 thruster shown in Fig. 3 is a modular construction to allow as many geometrical variations as possible. The thruster consists of a plenum chamber 70 mm in diameter, divided into five copper rings of similar size, and a backplate. The last three downstream rings can be connected as anode. The cathode, which is 220-mm long and 18 mm in diameter, is a 2% thoriated tungsten rod with a cast copper base. The displaceable cathode can be positioned during the experiment by a remotely controlled electromotor. The cathode is guided in a boron nitride pivot upstream in the water-cooled backplate. All parts except this ceramic pivot are individually water-cooled. Two propellant ports are placed in a slit around the cathode and at the anode radius respectively, both at the backplate.

III. Cathode Temperature and Current Density

The cathode temperature distribution has been determined by using the MPD device DTF shown in Fig. 2 with cathodes of 12-mm diameter.

The cathode temperature field was measured with a CID camera and a narrow (10 nm) bandpass interference filter, calibrated with a graphite cavity blackbody standard up to a temperature of 2600 K with an accuracy of ±1 K. The emissivity of tungsten shows both a wavelength and a temperature dependence.[20] Spectroscopic measurements showed that $\lambda = 959$ nm is a well-suited wavelength to make optical measurements with argon as propellant.

A series of tests were conducted with a 2% thoriated tungsten cathode to investigate the temporal behavior and its dependence on ambient pressure and mass flow rate. In Figs. 4 and 5 the temperature of the cathode is shown as a function of the distance to the cathode tip, measured during runs of about 8000 s each at a current level of 2000 A, with a mass flow rate of 1 g/s argon and an ambient pressure of 14 mbar for the first run, and 20 mbar for the second run. The first experiment (Fig. 4) was carried out with a new cathode. As can be seen, the tip temperature as well as the extent of the arc attachment zone increases with time even after a running time of over 2 h. The arc attachment zone can be seen clearly; it ends at a surface temperature of about 2600 K. From that point on, the cathode temperature decreases linearly, while there is a nonlinear decrease of temperature within the attachment zone.

For the second test the same cathode was used as for the first experiment, but now this cathode is no longer new. Figure 5 shows the cathode temperature distribution at various times. Almost no increase of the tip temperature can be detected, but the area of arc attachment increases as in case one. It seems that the substantial increase in the tip temperature during the first experiment was caused by a burn-in effect of the new cathode, whereas the increase in the attachment area with time may be explained by a thorium depletion which leads to a lower work function and therefore a lower current density. The ambient pressure and mass flow rate have almost no influence on the cathode tip temperature, which is in the range of 3000–3150 K for all cases, and on the temperature at the end of the arc attachment zone, which was found to be about 2600 K. However, the size of the attachment area is strongly affected, decreasing with increasing mass flow rate and pressure. Both cases can be explained by increasing convective cooling.

The average current density in the arc attachment zone of the cathode determined with the Richardson formula and the temperature distribution is plotted in Fig. 6 vs the mass flow rate of argon for two different ambient pressures with a total arc current of 2 kA. Since the attachment area is also a function of time, the moment of the measurement is indicated in the plot. The current density increases from 1500 kA/m^2 with 0.4 g/s argon to 2400 kA/m^2 with 1 g/s in the case of an ambient pressure of 14 mbar. The current density is higher at higher ambient pressures. At 20 mbar it increases from 2000 kA/m^2 with 0.4 g/s to 4000 kA/m^2 with 1 g/s.

In order to answer the question whether the electron emission of the hot glowing thoriated tungsten can be shown to be purely thermionic, a temperature profile was used to calculate the current density profile; the former was measured at 2 kA, $p = 14$ mbar and $\dot{m} = 1$ g/s, 480 s after ignition. For this purpose the Richardson formula was applied, using an emission constant A of 10^4 $A/(m^2K^2)$ and a work function of 2.6 eV determined by Bade and Yos[10] using a constant emissivity of 0.4. To get comparable results for the used temperature profile, the same emissivity value of 0.4 was employed. An integration of the current density over the arc attachment zone yields a total current of 2001 A. This result is in very good agreement with the measured current of 2050 A and seems to show that the electron emission is purely thermionic.

For the test depicted in Fig. 5, the change of the work function during the experiment was investigated, using again the Richardson formula with the same emission constant A of 10^4 $A/(m^2K^2)$, and the average current density and temperature. The work function increases from 2.49 eV at 364 s to 2.73 eV at 8000 s. It is in good agreement with the value of 2.6 given by Bade and Yos[10] for thoriated tungsten.

At the plasma wind tunnel PWK1-IRS, which is equipped with the plasma source RD2,[21] an optical glass window is available to measure the cathode tip temperature by py-

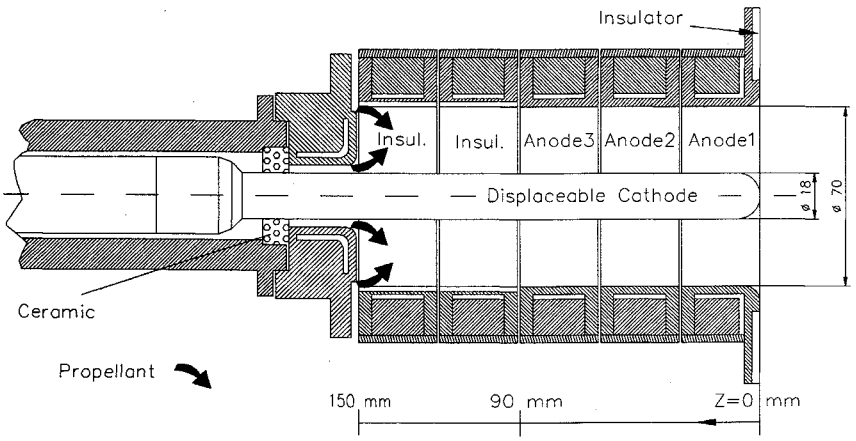

Fig. 3 Cylindrical MPD thruster ZT1.

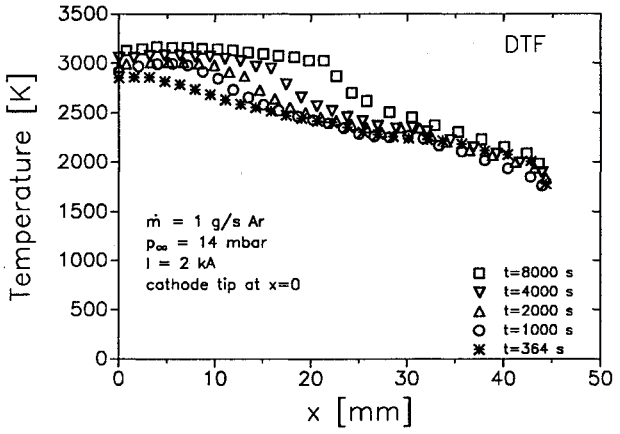

Fig. 4 Temperature of the cathode as a function of the distance to the cathode tip; experiment 1.

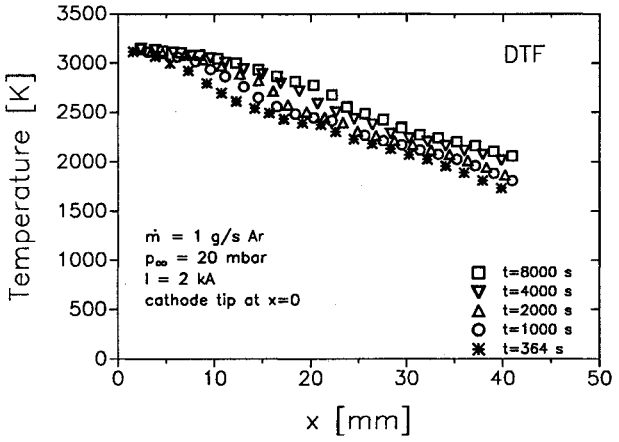

Fig. 5 Temperature of the cathode as a function of the distances to the cathode tip; experiment 2.

rometry. Therefore, this test stand was used to investigate the tip temperature dependence on current level and propellant by a linear pyrometer. N_2 and Ar were used as propellants.

Three different interference filters for cathode temperature measurement are available at the following wavelengths: 798, 888, and 959 nm. The temperature dependent emittance values at these wavelengths were taken to evaluate the data. Mass flow rates of 0.9 g/s in the case of Ar and 0.8 g/s in the case of N_2 were chosen to get roughly the same chamber pressure. The current was varied from 0.8 to 2 kA. Test series were carried out with a 2% thoriated tungsten cathode as well as with a 1% thoriated one. Whereas the cathode tip temperature increases clearly with argon as propellant, it is shown to be nearly constant with nitrogen and the 1% thoriated

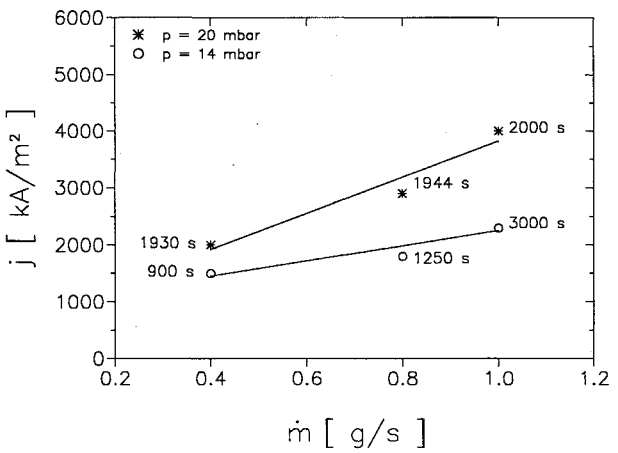

Fig. 6 Average current density as a function of mass flow.

Table 1 Current (I), mass flow rate ($\dot{m}$), chamber pressure (p_{ch}), and cathode tip temperature ($T_{c,tip}$) for a 1 and 2% thoriated tungsten cathode

	I, kA	$\dot{m}$, g/s	p_{ch}, mbar	$T_{c,tip}$, K
		1% ThO_2		
Ar	0.8	0.9	114	3012
	1.0		116	3118
	1.25		123	3287
	1.5		124	3404
	1.75		138	3453
	2.0		143	3535
N_2	0.8	0.8	—	—
	1.0		117	3303
	1.25		120	3306
	1.5		127	3276
	1.75		135	3303
	2.0		—	—
		2% ThO_2		
Ar	0.8	0.9	129	2949
	1.0		131	3055
	1.25		134	3165
	1.5		140	3230
	1.75		148	3293
	2.0		—	3319
N_2	0.8	0.8	125	3259
	1.0		127	3271
	1.25		135	3212
	1.5		141	3062
	1.75		145	3095
	2.0		—	—

material, and even a small decrease could be detected with the 2% thoriated tungsten cathode rod. Some results are listed in Table 1.

IV. Erosion Experiments

In a previous paper[12] the erosion of MPD devices was investigated systematically. It was shown that two different modes must be distinguished: (the old erosion rates of Ref. 12 in parentheses) 1) ignition phase (13 μg/C); 2) steady-state phase (0.03 μg/C).

The above mentioned values were obtained with uncleaned commercial welding argon. Some effects like a black coloring of the anode noticed during operation raised the suspicion that the propellant gas contained some traces of oxygen and/or water vapor. To avoid these possible oxidation effects, which also could augment erosion, in a new test series the welding argon was replaced by argon of purity grade 4.8 ($\cong$99.998%). Additionally, the gas was cleaned by a drying and deoxigenation process (Oxisorb, from Messer-Griesheim). With these means, new erosion rates were measured which are significantly lower than those quoted in Ref. 12.

A. Erosion During Ignition Phase

The ignition phase is characterized by a cold cathode and a highly unstable, spotty arc attachment. These "arc spots" jump irregularly over the cathode surface,[1] causing melting with relatively high erosion and leaving "craters" of sizes ranging from some microns to a tenth of a millimeter. This starting phase ends when the cathode is hot enough for thermionic emission to support the current demand. This is indicated by a sudden decrease in voltage together with an increase in current (power supply response), depicted in Fig. 7.

To determine the average erosion rate during this starting phase, experiments with single ignitions and series ignitions were performed. In each case, the arc was extinguished after stabilization. In the first case, the cathode was removed and weighed after each shot, in the second, the tank was held under vacuum during a series of 8–20 shots. To exclude possible thermal effects in the starting phase, a waiting period of about 10 min was taken between the tests to cool down the cathode.

Comparison of the results with measurements made using unpurified welding grade argon[12] demonstrates that the erosion rate during the ignition phase is insensitive to the gas purity. For example, an erosion rate of 13 μg/C previously measured with argon lies within the range of 8.4–15 μg/C measured using the purer argon. The fact that the single shot erosion rates are about half those of the series experiments is rather surprising. This could perhaps be caused by the influence of atmospheric oxygen. During the series experiments the cathode was not exposed to oxygen, preventing re-establishment of an oxide layer on the cathode surface. With the single shot tests, however, such a layer could have formed during weighing. Guile and Jüttner[22] found that with oxidized cathodes in vacuum discharges, the average size of the crater is smaller and the lifetimes are shorter, resulting in an erosion rate that is lower than with metallic surfaces. This could also be an explanation in our case.

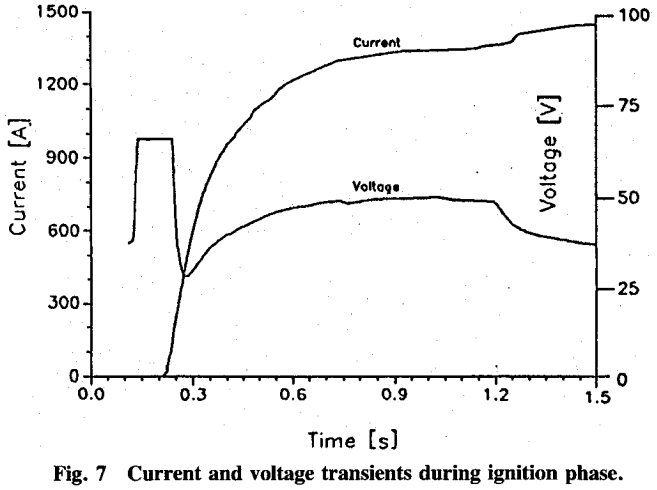

Fig. 7 Current and voltage transients during ignition phase.

Besides the normally used 2% thoriated tungsten material, a 1% thoriated tungsten material was also investigated. It showed no significant difference in erosion behavior from the standard cathode material.

B. Erosion During Steady-State Operation

The erosion during the steady-state phase was determined by means of long duration tests lasting about 2 h. The mass lost during startup was subtracted from the total measured weight change using the values measured for single shots. Contrary to the erosion during the starting phase, the mass loss is strongly influenced by the gas purity. After the installation of the deoxygenation device, the steady-state erosion could be lowered by a factor >20. The results of several test series are compiled in Table 2. The steady-state erosion rates of the 1% thoriated tungsten cathode also show no significant difference from the standard 2% ThO_2 material, ranging from 1 to 2 ng/C. The lowest values have been measured with nitrogen, the highest with hydrogen. The difference between the nitrogen and argon erosion rates may be explained by the higher cathode temperatures found with argon (Table 1).

Also included in Table 2 are the data obtained by a cathode which was used in the plasma generator RD2 for plasma wind-tunnel applications. There it accumulated a running time of 681×10^3 s (189 h) with 247 ignitions and a charge transfer of 748×10^6 C. The average mass loss per ignition was found to be 4.8 mg, yielding a total steady-state erosion rate of 2.1 ng/C, which is about 4 times higher than the value obtained from the MPD tests. This could be explained by the higher arc chamber pressure, which concentrates the arc attachment zone on the cathode, and therefore yields higher cathode temperatures and sublimation rates.

With a pure thermionic cathode, erosion is dominated by the sublimation rate s, which is calculated according to the modified Dushman equation derived in Ref. 12

$$s(T) = \frac{\dot{m}_{\text{subl}}}{I} = \sqrt{\frac{M}{2\pi\mathcal{R}T}}\frac{p_v(T)}{j}\left[\frac{kg}{C}\right]$$

where the vapor pressure p_v is calculated according to Ref. 23.

This sublimation rate is depicted in Fig. 8 as function of the cathode temperature with the current density as parameter. For a current density of $j = 5 \times 10^6$ A/m^2 and a temperature of 3000 K, the sublimation rate yields 2 ng/C, which corresponds well with the experiment.

C. Erosion Measurements with the SLA-Method

To confirm the weight loss measurements and study the temporal evolution of cathode erosion rates, the mass loss was also measured using an independent, time resolved method called surface layer activation method.[24] These tests were conducted with the thruster DTF-IRS shown in Fig. 2.

Figure 5 displays the cathode temperature evolution observed in the test which is discussed here. For the test a 2% thoriated tungsten cathode was used, the propellant flow rate was 1 g/s and the thruster was started with a tank pressure of 14 mbar and a current level of 1100 A, which was then increased to 2000 A. The tank pressure was rapidly increased to 20 mbar after the ignition and the thruster operated for 8500 s.

In addition to cathode weight loss measurements, the erosion was determined using a radioactive tracer in a thin surface layer on the cathode tip. Because this technique yields the

Table 2 Cathode erosion during continuous operation

Cathode material/∅	Propellant	Current, A	Chamber pressure, mbar	Erosion rate, ng/C
Thruster: DT2				
98% W, 2% ThO_2/12 mm	Ar	1500	94	1.39
		2000	110	1.66
		3000	130	1.28
	N_2	2000	84	0.59
		2000	98	0.58
	H_2	1000	59	2.21
98% W, 2% ThO_2/8 mm	N_2	1000	42	0.46
99% W, 1% ThO_2/12 mm	Ar	2000	84	1.90
Thruster: RD2				
98% W, 2% ThO_2/8 mm	N_2	1000	300–700	2.1
Thruster: DTF				
98% W, 2% ThO_2/12 mm	Ar	1500–2500	13–26	1.4–5.4

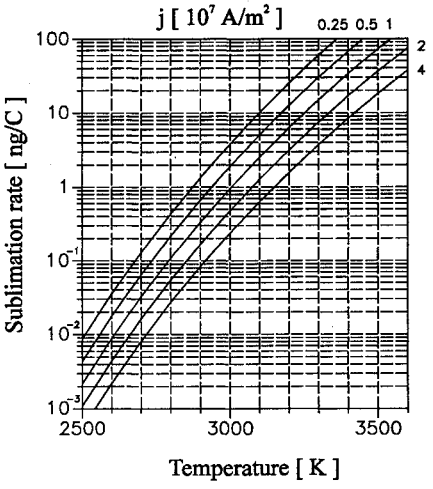

Fig. 8 Sublimation rates of tungsten as a function of the cathode temperature with the current density as a parameter.

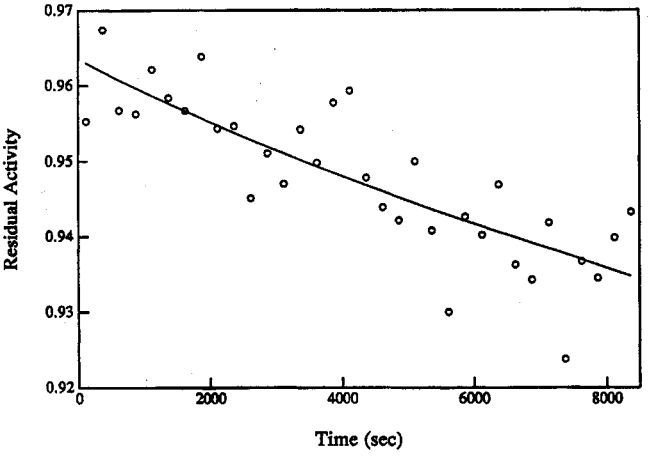

Fig. 9 Detector signal as a function of time; experiment 2.

erosion rate as a function of time, the startup erosion can be distinguished from the steady-state erosion. The gamma-emitting ^{184}Re tracer was produced by bombarding a 5-mm-diam spot on the tip of the cathode with a 15 MeV deuteron beam, transmuting a small fraction of the tungsten atoms. While this activated layer was eroded, the measured activity level decreased, and the mass loss per unit surface area was related to the fraction of activity remaining with a calibration curve. This integrated activity profile was measured on three tungsten samples activated under the same conditions used in the actual tests. The activity was monitored during the tests with a 3 × 3 in. NaI detector mounted in a water-cooled container under the thruster. The exemplary detector signal for experiment 2 (Fig. 5), which was amplified by a stabilized-gain amplifier and collected with a multichannel analyzer, is shown as a function of time in Fig. 9. The analysis of this data consists of fitting a function containing a model of the erosion rate as a function of time and a correction for changes in the calibration curve due to diffusion of the radioactive tracer into the cathode.

The temperature evolution curve of the test is drawn in Fig. 5. As can be seen, the tip temperature was approximately constant after a relatively short starting transient, and the area of the emitting zone increased only slightly during the experiment. Because the cathode mass loss is apparently dominated by evaporation of cathode material, the erosion rate model was chosen to follow the behavior of the evaporation rate for the observed temperatures. The set of data was fitted assuming a constant erosion rate, since the temperature was approximately constant.

In the described experiment, a total of 82.93 mg was lost from the cathode, which is an average rate of 4.87 ng/C. The surface layer activation technique yielded an erosion rate of 1.11×10^5 kg/(m²s) for the steady-state phase of operation, a mass loss per unit area of 0.0215 kg/m² for the startup phase, and a total mass loss per unit area of 0.1162 kg/m². The estimated emitting area was about 6.4×10^{-4} m², which gives a current density of 3100 kA/m² and an erosion rate of 4.4 ng/C, which is very close to the value determined independently by the weight loss.

Given the uncertainties in the data and the approximations required to convert to the same units, the SLA technique yields erosion rates that are surprisingly close to those determined by the weight loss. In addition to an independent verification of the erosion rates, the SLA data indicates that the mass loss is fundamentally related to the surface temperature.

V. High Current Damage

At high current densities within the cathode, severe problems have been encountered with all thruster geometries. Cracks releasing molten material from the interior appeared on the 2% thoriated tungsten cathodes. However, melting did not occur at the tip, where the heat transfer from the arc to the cathode is high and the maximum surface temperature was expected, but closer to the lower temperature end of the tungsten rod, where the cathode was blown up. As an example, Fig. 10 shows a cathode 18 mm in diameter and 45-mm long used within the thruster DT2 (Fig. 1) at about 6500 A. To clarify the reason for this behavior, some cathodes

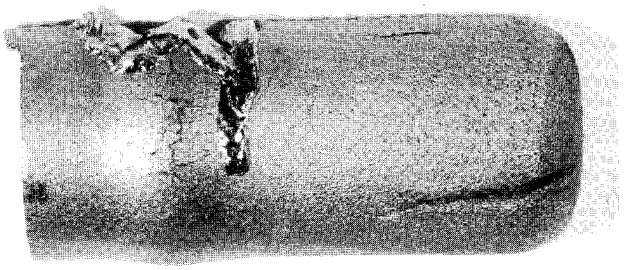

Fig. 10 Damaged cathode of thruster DT2.

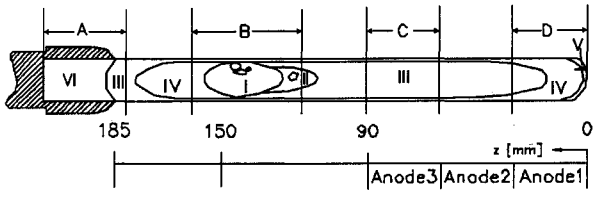

Fig. 11 Scheme of the cut through the damaged cathode ZT1.

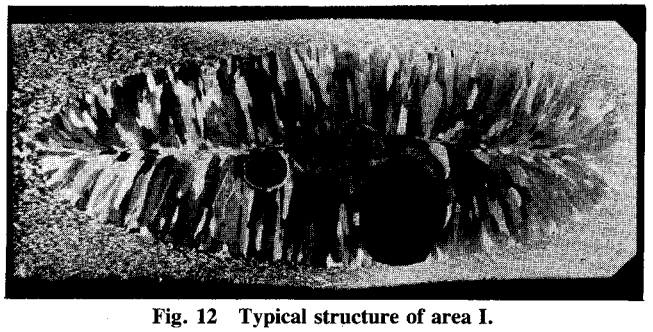

Fig. 12 Typical structure of area I.

have been investigated metallurgically at the Materialprüfungsanstalt (MPA) at the University of Stuttgart.

Metallographic cuts were prepared in longitudinal and transverse directions from the unaffected base material and from the damaged areas. They were investigated in a light microscope and in a scanning electron microscope (SEM) using secondary electrons, backscattered electrons and x-ray microanalysis (energy dispersive and wavelength dispersive, respectively).

In Fig. 11, the cut of a damaged cathode of ZT1 (Fig. 3) is drawn schematically. Six different areas (I–VI) were detected as the result of the investigations, each of them with a characteristic microstructure.

The material in area VI is comparable to unaffected material. It is characterized by a more or less homogeneous distribution of ThO_2 particles in the tungsten matrix. The diameters of the ThO_2 particles are up to about 1–10 μm in the transverse, and up to about 40 μm in the longitudinal directions. This preferential orientation is caused by the forging of the tungsten rod.

In area I (Fig. 12), the temperature reached its maximum and the material melted, forming voids of diameters of 2–6 mm. The inner surface of these voids is covered with a layer of pure thorium oxide with a thickness ranging from 0.05 mm up to 1 mm. The columnarly resolidified material is of pure tungsten and contains neither ThO_2 particles nor any detectable thorium or oxygen.

In the temperature region not much below the melting temperature (area II), recrystallization of the tungsten matrix occurs as well as a significant coarsening of the tungsten grains, with no indication of a longitudinal orientation. Furthermore, a nearly perfect spheroidization and a considerable coarsening of the ThO_2 particles to diameters up to about 0.1 mm are found (the black regions in Fig. 13). Area II is especially pronounced on the cathode tip side of the melted zone, and it is possibly a step which precedes the melting of the material.

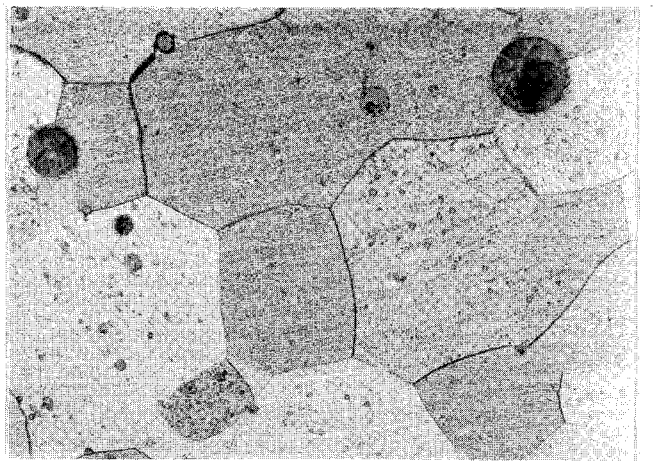

Fig. 13 Typical structure of area II.

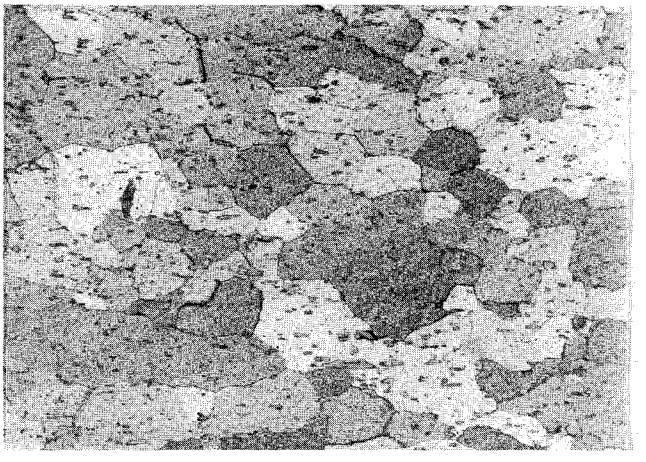

Fig. 14 Typical structure of area III.

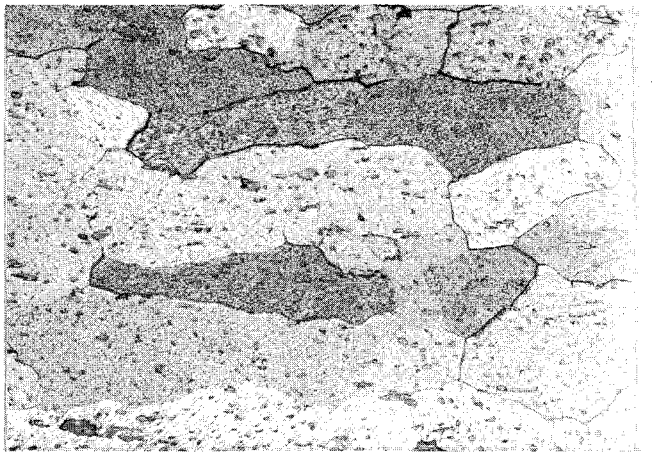

Fig. 15 Typical structure of area IV.

In Figs. 14 and 15, typical structures of area III and IV are depicted. In both areas, the ThO_2 particles are evenly distributed. They still exhibit an orientation parallel to the longitudinal direction, but they are beginning to develop a rounder shape. Whereas, recrystallization is beginning in area III, it is completed in area IV. Compared to area II and III, the grain size is considerably less in area IV.

So it can be concluded that the local temperature has been highest in area I, the melted region, followed by area II, then area IV, still lower in area III, and lowest in area VI. It is worthwhile to note that the area IV is extended over nearly all the cylindrical surface of the cathode.

With 8 kA the arc attachment on the cathode probably reaches the swollen region in section B. At that point, the current density within the cathode rod and therefore the ohmic heating reaches its maximum and causes the melting of the cathode material. This melting starts in the cathode center, due to the radiation cooling on the cathode surface.

At the tip of the cathode, area V, the tungsten material was found to be porous within the first 0.4 mm and no ThO_2 could be measured within this zone, whereas at the cylinder surface, no depletion of the ThO_2 and no porosity was detected. The main current attachment during the steady-state phase of operation occurs on the cylindrical part of the surface. Therefore, it seems that this porosity and depletion were created during the ignition phase.

VI. Conclusions

The described experiments lead to two main findings.

1) The erosion rate of a glowing cathode during continuous operation can be lowered to the sublimation rate by applying an oxygen-free propellant, so that cathode erosion will no longer constitute a lifetime limiting factor for missions using MPD propulsion. A further reduction of the erosion can only be reached by reduction of the cathode temperature.

2) The cathode operation is limited by the current density in the cathode shaft. Too high current densities lead to melting and destruction of the cathode. This phenomenon seems to be evoked or at least influenced by the thoria distribution. A possible remedy may be the use of cathodes with lower contents of thoria and in shaping the cathode to avoid too high current densities in still very hot cathode zones, i.e., directly behind the current attachment zone.

Acknowledgments

This work was supported by the Air Force Office of Scientific Research Grants AFOSR-86-0337, AFOSR-88-0325 and AFOSR-89-0535. This support is greatly appreciated.

References

[1]Schrade, H. O., Auweter-Kurtz, M., and Kurtz, H. L., "Cathode Phenomena in Plasma Thrusters," *Proceedings of the 19th IEPC*, Colorado Springs, CO, 1987 (AIAA Paper 87-1096).

[2]Yoshikawa, T., Kagaya, Y., and Kuriki, K., "Thrust and Efficiency of New K-III MPD Thruster," *Proceedings of the 16th IEPC*, New Orleans, LA, 1982 (AIAA Paper 82-1887).

[3]Kuriki, K., et al., "MPD Arcjet System Performance Test," International Astronautical Federation Preprint 83-392, 34th IAF Congress, Budapest, Hungary, 1983.

[4]Clark, K. E., and Jahn, R. G., "Magnetoplasmadynamic Thruster, Erosion Studies, Phase I," Interim Rept., U.S. Air Force Contract R 04611-79-C-0039, April 1983.

[5]Schrade, H. O., Auweter-Kurtz, M., and Kurtz, H. L., "Analysis of the Cathode Spot of Metal Vapor Arcs," *IEEE Transactions on Plasma Science*, Vol. PS-11, No. 3, 1983, pp. 103–109.

[6]Daalder, J. E., "Diameter and Current Density of Single and Multiple Cathode Discharges in Vacuum," *IEEE Transactions on Power Apparatus and System*, Vol. PAS-93, 1974, pp. 1747–1758.

[7]Bushik, A. I., Jüttner, B., Pursch, H., and Shilov, A., "Effects of Local Heat Accumulation at the Cathode of Vacuum Arcs," Preprint: Akademie der Wissenschaften der DDR, Zentralinstitut für Elektronenphysik, Feb. 1983.

[8]Rakhovskii, V. T., "Experimental Study of the Dynamics of Cathode Spot Development," *IEEE-Transactions on Plasma Science*, Vol. PS-4, No. 2, 1976, p. 81.

[9]Hügel, H., and Krülle, G., "Phänomenologie und Energiebilanz von Lichtbogenkathoden bei niedrigen Drücken und hohen Stromstärken," *Beiträge der Plasmaphysik*, Vol. 9, 1969, pp. 87–116.

[10]Bade, W. L., and Yos, J. M., "Theoretical and Experimental Investigation of Arc Plasma-Generation Technology," *Technical Documentary Report* ASD-TDR-62-729, Pt. II, Vol. 1, Air Force Materials Lab., Wright-Patterson AFB, OH, 1963.

[11]Sovey, J. S., and Mantenieks, M. A., "Performance and Lifetime Assessment of MPD Arc Thruster Technology," *Proceedings of the 24th Joint Propulsion Conference*, Boston, MA, 1988 (AIAA Paper 88-3211).

[12]Schrade, H. O., Auweter-Kurtz, M., and Kurtz, H. L., "Cathode Erosion Studies on MPD Thrusters," *AIAA Journal*, Vol. 25, No. 8, 1987, pp. 1105–1112.

[13]Myers, R. M., "Energy Deposition in Low Power Coaxial Plasma Thrusters," Ph.D. Dissertation, Dept. of Mechanical and Aerospace Engineering, Princeton Univ., Princeton, NJ, 1989.

[14]Sokolowski, W., O'Donnell, T., and Deininger, W. D., "Cathode and Insulator Materials for a 30 kW Arcjet Thruster," *Proceedings of the 25th Joint Propulsion Conference*, Monterey, CA, 1989 (AIAA Paper 89-2514).

[15]Donaldson, A. L., and Kristiansen, M., "An Assessment of Erosion Resistant Cathode Materials with Potential Applications in High Power Electric Propulsion Devices," *Proceedings of the 25th Joint Propulsion Conference*, Monterey, CA, 1989 (AIAA Paper 89-2515).

[16]Polk, J. E., Kelly, A. J., and Jahn, R. G., "MPD Thruster Erosion Research," *Proceedings of the 19th International Electric Propulsion Conference*, Colorado Springs, CO, 1987 (AIAA Paper 87-0999).

[17]Wegmann, T., Auweter-Kurtz, M., Kurtz, H., Merke, W., and Schrade, H. O., "Steady State High Power MPD Thruster Design," *Proceedings of the 21st IEPC*, Orlando, FL, 1990 (AIAA Paper 90-2555).

[18]Auweter-Kurtz, M., Habiger, H., Laure, S., Messerschmid, E., and Schönemann, A., "Experimental Investigations of MPD Devices Used as Reentry Test Plasma Sources," *Proceedings of the 21st IEPC*, Orlando, FL, 1990 (AIAA Paper 90-2570).

[19]Kurtz, H. L., Auweter-Kurtz, M., Glocker, B., Habiger, H., Merke, W., and Schrade, H. O., "Cylindrical Steady-State MPD Thruster," *Proceedings of the 20th IEPC*, DGLR Bericht 88-02, Bonn, Germany, 1988, pp. 153–162.

[20]Touloukian, Y. S., and DeWitt, D. P., "Thermophysical Properties of Matter," *Thermal Radiative Properties, Metallic Elements and Alloys*, Vol. 7, IFI/Plenum, New York, 1970.

[21]Auweter-Kurtz, M., et al., "Plasma Wind Tunnels PWK1, PWK2," *Internal Report*, Inst. für Raumfahrtsysteme, Univ. Stuttgart, IRS 89-P14, 1989.

[22]Guile, A. E., and Jüttner, B., "Basic Erosion Processes of Oxidized and Clean Metal Cathodes by Electric Arcs," *IEEE Transactions on Plasma Science*, Vol. PS-8, No. 3, Sept. 1980, pp. 259–269.

[23]Weast, R. C. (ed.), "*Handbook of Chemistry and Physics*," 51st Ed., The Chemical Rubber Co., Cleveland, OH, 1971.

[24]Polk, J., Kelly, A., Jahn, R., Kurtz, H., Schrade, H., and Auweter-Kurtz, M., "Mechanisms of Hot Cathode Erosion in MPD Thrusters," *Proceedings of the 21st IEPC*, Orlando, FL, July 1990 (AIAA Paper 90-2673).